ELSEVIER

Coordination Chemistry Reviews
197 (2000) 51–69

COORDINATION CHEMISTRY REVIEWS

www.elsevier.com/locate/ccr

Improving our understanding of molecular geometry and the VSEPR model through the ligand close-packing model and the analysis of electron density distributions

Ronald J. Gillespie *

Department of Chemistry, McMaster University, 1280 Main Street West, Hamilton, Ont., Canada

Received 26 March 1999; accepted 25 May 1999

Contents

* Tel.: +1-905-525-9140; fax: +1-905-522-2509.
E-mail address: gillespi@mcmaster.ca (R.J. Gillespie)

PII: S0010-8545(99)00199-X

Abstract

Considerable improvements in our understanding of molecular geometry have been made in recent years as a result of the recognition in the ligand close-packing (LCP) model of the importance of ligand–ligand repulsions and the information gained by the study of electron density distributions. These improvements have enabled several aspects of the VSEPR model to be better understood and explanations of exceptions to the model to be proposed. The LCP model shows that particularly for the small atoms of the period 2 elements, ligand–ligand interactions are very important in determining geometry. For example LCP is the reason for the nonVSEPR octahedral geometry of molecules such as $SeCl_6^{2-}$. Atomic charges determined from electron density distributions affect the size of a ligand atom which can therefore change from molecule to molecule and allowance for this must be made in applying the LCP model. Electron density distributions also enable us to find the shape of a ligand which is such that in $B(OH)_4^-$, for example, the bond angles at boron deviate considerably from the tetrahedral angles.

Keywords: VSEPR model; Molecular geometry; Ligand–ligand repulsions; LCP model

1. Introduction

Considerable improvements in our understanding of molecular geometry have been made in recent years as a result of the recognition in the LCP model of the importance of ligand–ligand repulsions and the study of electron density distributions. These improvements have enabled several aspects of the VSEPR model to be better understood and explanations of exceptions to the model to be given. In this paper I review these new developments and their relation to the VSEPR model.

First I briefly review the physical basis of the VSEPR model [1,2]. According to this model the electron pairs in the valence shell of the Lewis diagram for a molecule adopt those arrangements that keep them as far apart as possible, namely two pairs linear, three pairs equilateral triangular, four pairs tetrahedral, and so on. Because electrons do not occupy precise positions we can only find their most probable locations. These are a consequence of the Pauli principle according to which, same spin electrons have a maximum probability of being found as far apart as possible. In the common case of a valence shell consisting of eight electrons there are four electrons of α spin and four of β spin (Fig. 1) which each have a most probable tetrahedral arrangement. In a free atom or ion with eight valence shell electrons these two tetrahedra can adopt any relative orientation and there is an equal probability of finding an electron anywhere in the valence shell. In other words the atom has a spherical electron density distribution. In a molecule AX_n the attraction of the electrons of A by the ligands X enhances the probability of finding a pair of electrons of opposite spin between A and X. If there are two or more ligands and if they attract the electrons of A sufficiently strongly to overcome the electrostatic repulsion between the electrons, there is an enhanced probability of finding a pair of electrons of opposite spin in the bonding region between A and X.

Because of the correlation of the motion of same spin electrons there is also an enhanced probability of finding a pair of electrons in the other tetrahedral positions, that is in the lone pair regions. In other words, the valence shell electrons are partially localized into pairs. If this localization were complete each pair of electrons would be localized into its own region of space called its domain and there would be four such domains with a tetrahedral arrangement. Similar considerations apply to molecules in which there are five, six and even more valence shell electron pairs in the Lewis diagram of the molecule. The correlation of the motions of same spin electrons due to the Pauli principle is the basis of the VSEPR model.

2. Ligand–ligand interactions

Although it is widely recognized that the packing of molecules and ions determines the structures of many crystals it has not been so commonly recognized that the packing of the ligands around a central atom determines the geometry of many molecules. An extensive study of interligand distances in a wide variety of AX_n molecules [3,4], in which A is from the second period, revealed that the distance

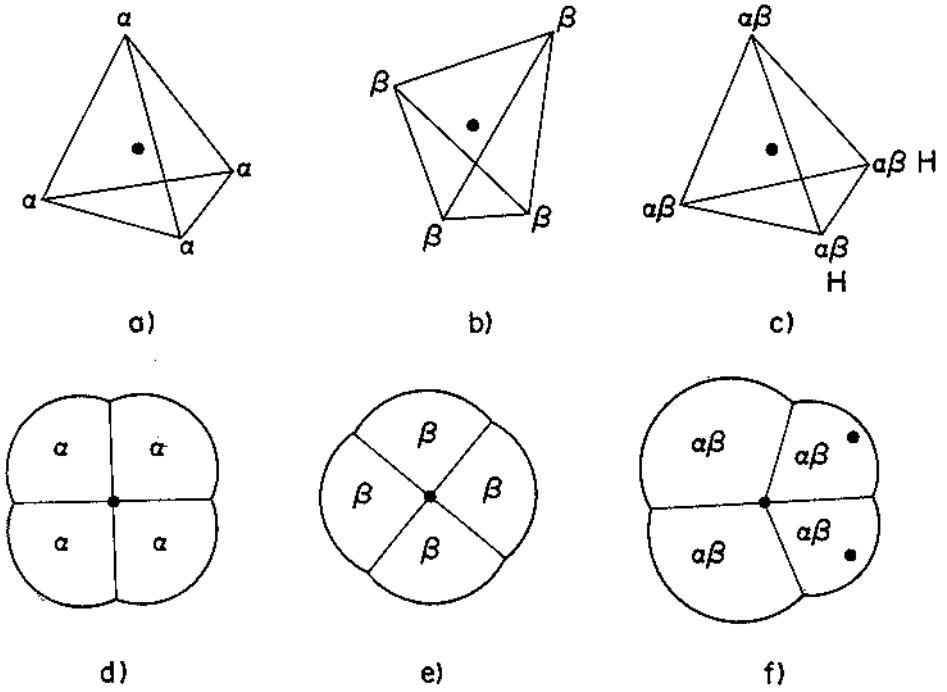

Fig. 1. Most probable arrangements of four valence shell electrons with spin α (a) and spin β (b), and of eight valence shell electrons in an AH_2 molecule (c). Two-dimensional representations of the domains of four valence shell electrons with spin α (d) and spin β (e), and of eight valence shell electrons (f) in an AH_2 molecule.

Table 1
Bond lengths, bond angles, and F···F distances in BF_n and CF_n groups [a]

	Coord. Number	A–F (pm)	<FAF (°)	F···F (pm)
F_2BF	3	130.7	120	226
F_2BOH	3	132.3	118.0	227
F_2BNH_2	3	132.5	117.9	227
F_2BCl	3	131.5	118.1	226
F_2BBF_2	3	131.7	117.2	225
F_3BF^-	4	138.2	109.5	226
F_3BNMe_3	4	137.2	111.5	229
$F_3BCH_3^-$	4	142.4	105.4	227
$F_3BCF_3^-$	4	139.1	109.9	228
			Mean	227
CF_3^+ [b]	3	124.4	120	216
$F_2C{=}CH_2$	3	132.4	109.4	216
$F_2C{=}CF_2$	3	133.6	109.2	218
F_2CO	3	131.9	107.6	216
F_3CF	4	131.9	109.5	216
F_3CO^-	4	139.2	101.3	215
F_3CCl	4	132.5	108.6	215
F_3COF	4	131.9	109.4	215
CF_3^- [b]	4 [c]	141.7	99.5	216
			Mean	216

[a] For the original references to the experimental data in Tables 1–6 see Refs. [3–5].
[b] Calculated structures.
[c] Includes lone pair.

between two given ligands is remarkably constant for a given A and is independent of the coordination number, bond length and bond angles, and of the presence of other ligands. Some examples are given in Table 1.

2.1. The ligand close-packing model

The observation that the intramolecular distance between two given ligands in these molecules is very nearly constant from molecule to molecule, suggests that the ligands can be thought of as hard objects tightly packed around the central atom A. This model is called the ligand close-packing (LCP) model [5]. To a good approximation the ligands can be regarded as hard spheres with a portion cut off to give a flat face in the bonding direction, as in the familiar space-filling models. Each ligand can then be assigned a radius called the intramolecular ligand radius, or simply the ligand radius. The distance between any two ligands is then given by the sum of the appropriate ligand radii. The radius of a given ligand depends on the nature of the central atom A because the difference in electronegativities between A and X determines the charge on X which in turn determines its size, that is its ligand radius. The ligand radius decreases with decreasing negative charge from a value approaching the crystal ionic radius [6] when the charge is close to the full

ionic radius. The ligand radii of several common ligands are given in Table 2 where we see that the ligand radius of a given ligand decreases from left to right across the periodic table as the electronegativity of the central atom A increases and the ligand charge decreases. For example, the ligand radius of fluorine bonded to beryllium, boron and carbon decreases from 128 to 113 to 108 pm which correlates well with the calculated charges on fluorine which are -0.88 in BeF_2, -0.81 in BF_3 and -0.61 in CF_4 [3].

That ligands may, to a good approximation, be regarded as hard spheres was first suggested by Bartell [7,8] for some organic molecules. He found that the bond angles in a variety of simple molecules could be explained by the packing of ligands of a given radius around a central carbon atom. As would be expected the radii for ligands bonded to carbon agree well with Bartell's radii (Table 2). This idea was taken up by several other authors, particularly Glidewell [9] who expanded Bartell's radii to other ligands and also to other molecules in which the central atom was not carbon. The radii determined by Bartell and Glidewell are often called 1,3 radii. However, the success of this earlier model was limited because these authors assigned only one fixed radius to a ligand not realizing that the radius of a ligand depends on the atom to which it is bonded.

2.2. Bond lengths and coordination number

For AX_n molecules with no lone pairs the VSEPR model and the LCP model both predict the same geometries, namely AX_3 equilateral triangular, AX_4 tetrahedral, AX_5, trigonal bipyramidal and AX_6 octahedral. However, the LCP model also predicts that bond lengths increase with increasing coordination number as we can

Table 2
Ligand radii (pm)

Ligand	Anion	Central Atom			Bartell
		Be	B	C	
C			137	126	125
O	140	134	120	114	114
F	136	128	113	108	108
Cl	181	168	151	144	144

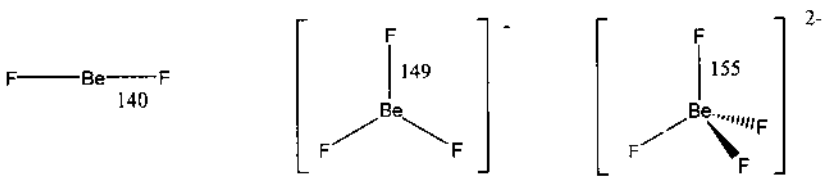

Fig. 2. Bond lengths (pm) in BeF_2, BeF_3^-, and BeF_4^{2-} showing the increase in bond length with coordination number.

see in Table 1 and Fig. 2. Three ligands can pack more closely than four which in turn can pack more closely than six, so for a given ligand the bond length increases with coordination number. Two ligands are not restricted by packing and so have an even shorter bond length (Fig. 2).

2.3. Bond angles in molecules with lone pairs and different ligands

In molecules of the type AX_nE_m where E is a localized lone pair, the lone pair domains occupy part of the valence shell thus preventing the ligands from occupying this region of the valence shell. The lone pairs can therefore be regarded as pseudo ligands so that the predicted AX_2E, AX_3E and AX_2E_2 geometries are the same as predicted by the VSEPR model. Because of the tendency of the lone pair density to spread out as much as possible the ligands are generally pushed into contact giving the same intramolecular distances as in AX_3 and AX_4 molecules. On the basis of the assumption that lone pair domains are larger than bonding pair domains, the VSEPR model predicts that in the presence of a lone pair the bond angles will be smaller than in the corresponding regular polyhedron, for example smaller than 109.5° in an AX_3E molecule and smaller than 90° in an AX_5E molecule but no prediction of the interligand distance of the bond lengths can be made. The LCP model, however, enables the interligand distances in such molecules to be predicted and the magnitude of bond angles to be understood. In general the longer are two adjacent bonds the smaller is the angle between them.

In accordance with the LCP model interligand distances in molecules with two or more different ligands are equal to, or close to, the sum of the appropriate ligand radii, so the relative sizes of bond angles can be understood and bond angles can be predicted if the relevant bond lengths are known. Some examples are given in Tables 3 and 4. This model provides a simple explanation of the initially surprising observation that the bond angles in HOX molecules are smaller than in both the H_2O and the X_2O molecules (Fig. 3). The small angle in the XOH molecules is a consequence of the constant interligand distance and the different bond lengths. Such predictions cannot be made by the VSEPR model.

Table 3
O···F interligand distances in some oxofluorocarbon molecules

	Bond length (pm)		Bond angle (°)	O···F (pm)
	C–F	C–O	FCO	
CF_3OCF_3	132.7	136.9	110.2	221
CF_3O^-	139.2	122.7	116.2	223
CF_3OF	131.9	139.5	109.6	223
COF_2	131.7	117.0	126.2	223
CH_3COF	134.2	118.1	121.4	223
FCO·OF	132.4	117.0	126.5	223
FOCCOF	132.9	118.0	124.2	223
			Sum of ligand radii	222

Table 4
Interligand distances in the chlorofluoromethanes

	Bond length (pm)		Bond angle (°)			X···X (pm)	
						Obs.	Pred.
CCl_4	CCl	177.1	ClCCl	109.5	Cl···Cl	289	290
$CFCl_3$	CCl	176	ClCCl	109.7	Cl···Cl	291	290
	CF	133	ClCF	109.3	Cl···F	253	253
CF_2Cl_2	CCl	174.4	ClCCl	112.5	Cl···Cl	290	290
	CF	134.5	ClCF	109.5	Cl···F	253	253
			FCF	106.2	F···F	215	216
CF_3Cl	CCl	175.1	FCCl	110.4	Cl···F	254	253
	CF	132.8	FCF	108.6	F···F	216	216
CF_4	CF	131.9	FCF	109.5	F···F	215	216

2.4. Nontetrahedral AX_4 molecules

A recent interesting application of the LCP model has been to provide an explanation of the nontetrahedral bond angles that are found in AX_4 molecules when X is a polyatomic ligand such as OY, NY_2 and CX_2Y [3,10]. These molecules do not have a truly tetrahedral geometry but always have S_4 or D_{2d} symmetry (Fig. 4). Even though the AX bonds are all the same length, four of the bond angles are larger than tetrahedral and two angles smaller than tetrahedral or four angles smaller and two larger. Some examples are given in Table 5. This unexpected geometry cannot be explained by the VSEPR model but is accounted for by the LCP model. The electron density distribution of a monatomic ligand is symmetric around the bond axis so that it makes contact with neighboring ligands at the same distance in any direction. In contrast, in any nonlinear polyatomic ligand such as

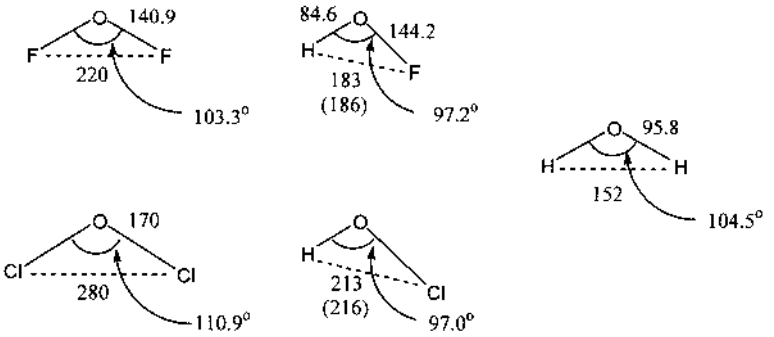

Fig. 3. Bond lengths (pm), bond angles, and interligand distances (pm) for F_2O, FOH, Cl_2O, ClOH and H_2O. The interligand distances in parentheses are the values predicted from the sum of the appropriate ligand radii.

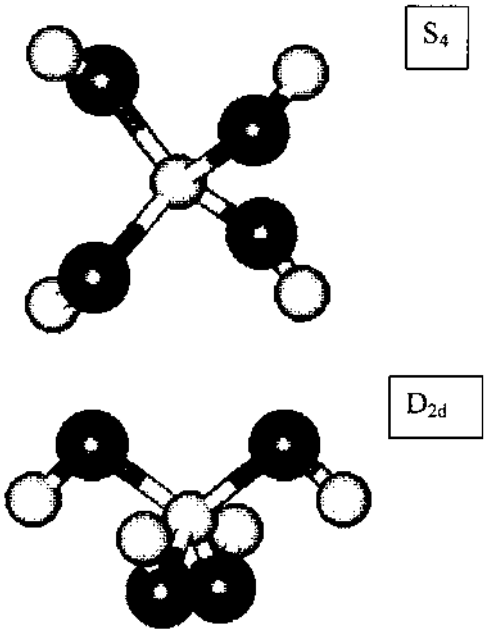

Fig. 4. The geometry of the S_4 and D_{2d} forms of $C(OH)_4$.

OX, NX_2, and CX_2Y the distribution of density around the O, N or C atom is not axially symmetric, so it makes contact with neighboring ligands at different distances in different directions. It has been shown that the closest possible packing of four such ligands around the central atom cannot be achieved with six tetrahedral bond angles around the central atom but only when the molecule has S_4 or D_{2d} symmetry [10]. In both these geometries there are four equal contact distances and two others that are equal to each other but different from the other four. Thus,

Table 5
Symmetries and bond angles for some $A(XY)_4$ molecules

	Symmetry	Bond Angles XAX (°)	
$B(OH)_4^-$ [a]	D_{2d}	106.2×2	111.1×4
$B(OMe)_4^-$	D_{2d}	101.7×2	113.5×4
$C(OH)_4$ [a]	S_4	107.2×4	114.2×2
$C(OMe)_4$	S_4	106.9×4	114.6×2
$C(CH_2Cl)_4$	S_4	106.1×2	112.9×2
	D_{2d}	108.3×4	119.2×2
$C(CH_2CH_3)_4$	S_4	108.6×2	109.9×4
	D_{2d}	106.7×4	110.9×2
$Ti(NMe_2)_4$	S_4	107.2×4	114.2×2
$V(O^tBu)_4$	S_4	106.7×4	115.1×2

[a] Calculated structures.

Table 6
Bond angles and bond lengths in some NX_3E and OX_2E_2 molecules

	N–X (pm)	XNX (°)		O–X (pm)	XOX (°)
NH_3	101.5	107.2	H_2O	95.8	104.3
NF_3	136.5	102.3	F_2O	140.9	103.3
NCl_3	175	106.8	Cl_2O	170.0	110.9
$N(CH_3)_3$	145.8	110.9	$(CH_3)_2O$	141.0	111.7
$N(CF_3)_3$	142.6	117.9	$(SiH_3)_2O$	163.4	144.1
$N(SiH_3)$	173.4	120.0	$(Me_3Si)_2O$	163	148
			Li_2O	160	180

there is set of four equal bond angles and another set of two equal bond angles neither of which is equal to the tetrahedral angle.

2.5. Weakly electronegative ligands

When the ligands X are appreciably less electronegative than the central atom A, the valence electrons of A are not well localized into pairs and their influence on the geometry of the molecule is weak so that ligand–ligand repulsions dominate, giving bond angles in AX_2E_2 and AX_3E molecules that are larger than tetrahedral and may reach 180° in OX_2E_2 molecules and 120° in AX_3E molecules (Table 6). In the limiting case of very weakly electronegative ligands, the central atom is essentially an A^{2-} or A^{3-} negative ion and the geometry of the molecule is dominated by ligand–ligand repulsions giving a linear molecule as in the case of Li_2O or a planar molecule as in the case of $N(SiH_3)_3$. Disiloxane $O(SiH_3)_2$ represents an intermediate situation in which the poorly localized nonbonding electrons exert just a weak effect on the geometry giving a large bond angle of 140° [11]. The VSEPR description of these molecules as AX_2E_2 and AX_3E is therefore not strictly valid when the ligands X are very weakly electronegative because the well localized lone pairs denoted by E are not present. In a molecule such as Li_2O the ligands cannot be said to be close-packed but nevertheless the geometry is determined by ligand–ligand repulsions.

2.6. Ligand–ligand interactions in molecules of period 3–6 elements

Because the bonds in these molecules are longer and weaker than those in the corresponding period 2 molecules, the ligands are not attracted so strongly to the central atom and so are not packed so tightly together. They can be regarded as being somewhat softer and more compressible than the same ligand in a period 2 molecule so they have a more variable ligand radius and consequently, the interligand distances are somewhat more variable and in particular increase somewhat with decreasing coordination number. This aspect of the LCP model has yet to be fully explored. Nevertheless, the LCP model is still useful because ligand–ligand interactions are still important in the molecules of period 3 and beyond as we see in the next section.

2.7. Stereochemically inactive and weakly active lone pairs

Some AX_6E molecules, such as $SeCl_6^{2-}$ and BrF_6^-, are exceptions to the VSEPR model because they have octahedral structures. The VSEPR model predicts that they should have a structure based on an arrangement of seven electron pairs which cannot lead to an octahedral geometry for the six ligands. In these molecules the lone pair is sometimes said to be stereochemically inactive because the octahedral geometry would be predicted if the lone pair were not present. This nonVSEPR geometry can, however, be easily understood in terms of the packing of the ligands around the central atom repulsions. In these molecules when six ligands are close-packed around the central atom no room is left for the lone pair which remains around the core of the central atom in a spherical distribution (Fig. 5). In fact it can no longer be described as a lone pair but only as a nonbonding pair of electrons which, having a spherical distribution, does not affect the geometry. The two nonbonding electrons do, however, show their presence by increasing the size of the central atom thereby giving unusually long bonds of 241 pm in $SeCl_6^{2-}$ compared with 216 pm for the length of the Se–Cl bond in $SeCl_2$ [3].

With a smaller ligand such as fluorine the six ligands in SeF_6^{2-} do not take up all the space in the valence shell of the central atom leaving some space for a lone pair. However, the remaining space is generally not large enough to accommodate a fully developed lone pair. So the two nonbonding electrons are located partially around the core of the central atom and partially in the valence shell forming what might be called a partial or 'weak' lone pair. This partial lone pair exerts only a weak distorting effect, so that the six ligands are only slightly distorted from an octahedral arrangement giving a C_{3v} geometry with three longer bonds and large bond angles surrounding the position of the partial lone pair and six shorter bonds forming smaller bond angles (Fig. 5) [12].

3. The analysis of electron density distributions

Recent developments in computers, particularly great increases in speed and memory, and a considerable decrease in their cost, have led to ab initio calculations of molecular wave functions and electron density distributions becoming almost routine procedures. The electron density distribution can be analyzed by the Atoms in Molecules (AIM) method [13] to provide much useful information about bonding and structure which has further enhanced our understanding of the VSEPR model and its limitations. In our discussion of the LCP model we referred to the nonaxially symmetric electron density distributions of ligands such as OH which distorts molecules such as $C(OH)_4$ from a truly tetrahedral geometry, and to atomic charges which, as we will see, are obtained from the analysis of electron density distributions. Electron density distributions can be conveniently presented in the form of contour maps of the electron density, ρ. Two typical electron density contour maps, that for the linear molecule $MgCl_2$ and that for the angular SCl_2 molecule are given in Fig. 6.

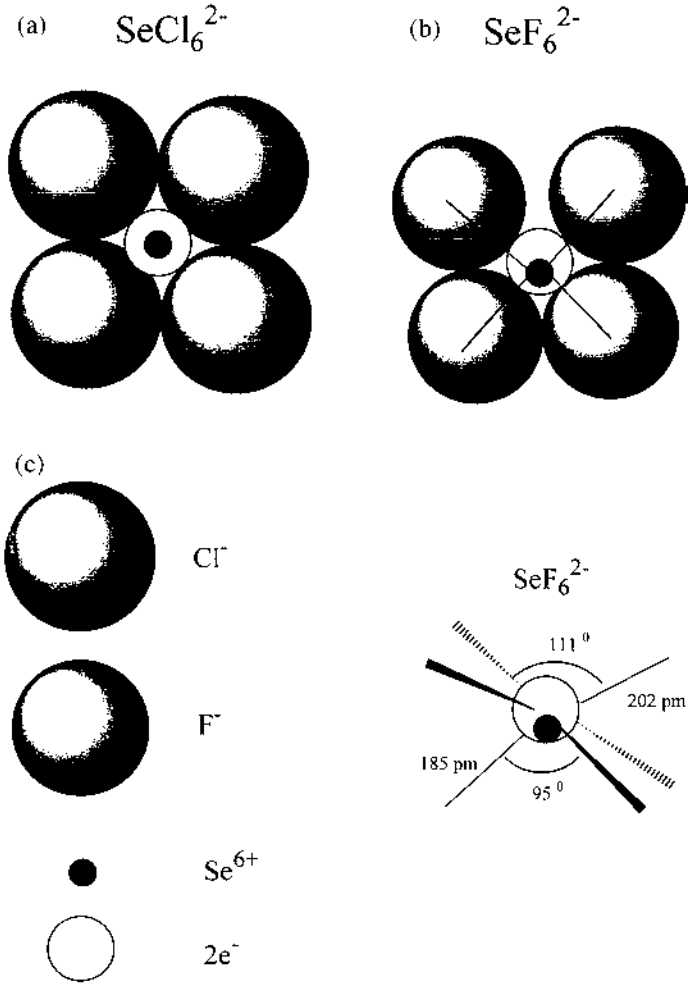

Fig. 5. (a) A view of a mirror plane of the octahedral $SeCl_6^{2-}$ ion showing the close-packing of four Cl^- ions around a central Se_4^{2+} ion consisting of an Se_6^{+} core surrounded by two nonbonding electrons. (b) A view of a possible C_{2v} distortion of an octahedral SeF_6^{2-} ion to illustrate the effect of a lone pair that only partly occupies the valence shell. (c) The observed C_{3v} geometry of the SeF_6^{2-} ion.

3.1. The bond path

We see in Fig. 6 that in both $MgCl_2$ and SCl_2 a very large part of the electron density, ρ, is concentrated in an almost spherical distribution around each nucleus and that the density in the outer regions of each atom, that is in the valency region, is relatively very small. In both molecules there is a deviation from a spherical distribution in the outer regions of each atom, although this is hardly noticeable in $MgCl_2$. In the contour map for SCl_2 we see more clearly that the electron density

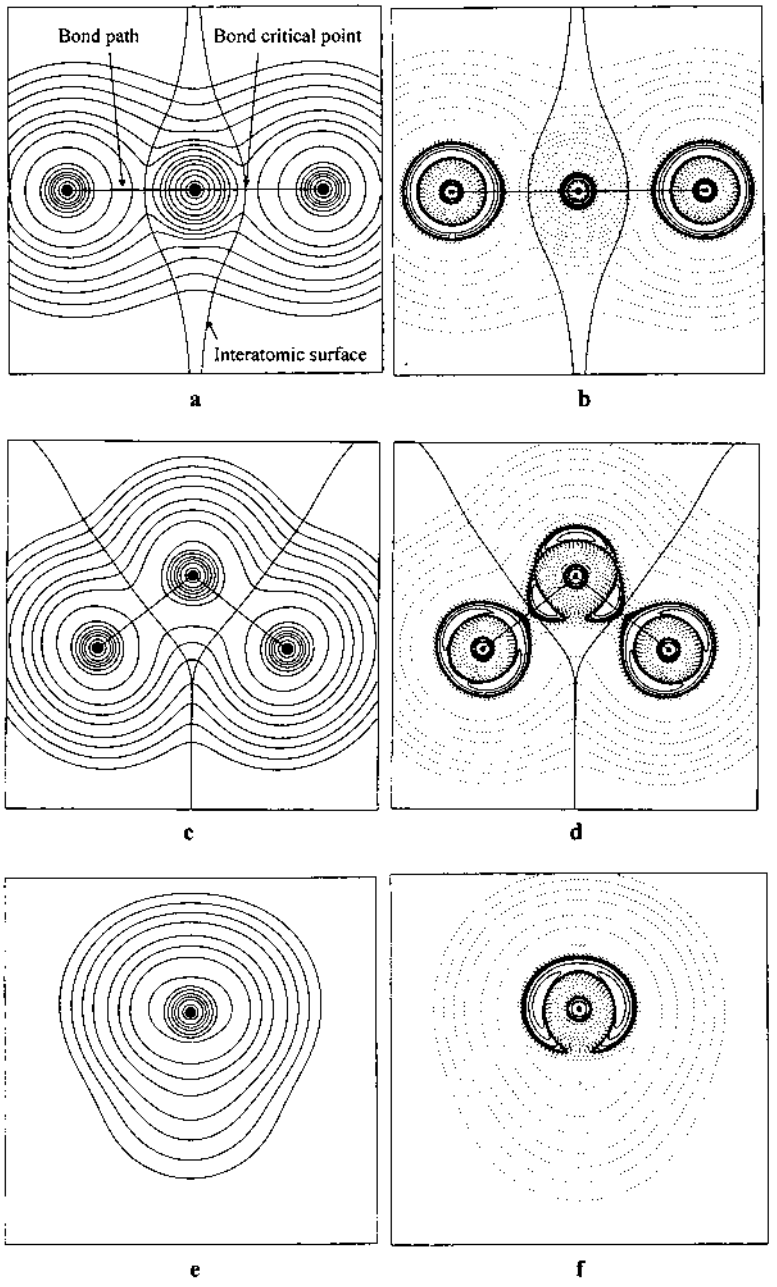

Fig. 6. Contour maps of ρ (a) and $L(r)$ (b) for the $MgCl_2$ molecule. Contour maps of ρ (c) and $L(r)$ (d) in the plane of the SCl_2 molecule. Contour maps of ρ (e) and $L(r)$ for the σ_v plane of the SCl_2 molecule. The outermost contour has the value 0.001 a.u. and the other contours moving inwards the values 2×10^n, 4×10^n, 8×10^n a.u., with n having the increasing values -3, -2, -1... For ρ 1 a.u. = e Bohr^{-3}, for $L(r)$ 1 a.u. = e Bohr^{-5}.

of an atom is stretched out towards each atom to which it is bonded and is accumulated along a line joining the two atoms. In any direction perpendicular to this line the electron density decreases but along this line it reaches a maximum at each nucleus and a minimum value at some point in between. This line is called a bond path and is found between every pair of atoms that chemists usually consider to be held together by a chemical bond. The point of minimum density along the bond path is called the bond critical point and the value of the density ρ at this point is called the bond critical point density, ρ_b. This quantity gives an indication of the amount of density accumulated in the bonding region.

3.2. The interatomic surface and atomic charges

Another important feature of the density is that a surface, called the interatomic surface, can be defined such that it separates the electron density belonging to one atom from that of its neighbor. We do not need here to go into the exact topological definition of this surface which is discussed in Ref. [12]. Looking at a two-dimensional contour map such as that for SCl_2 (Fig. 6) we see the line along which each interatomic surface cuts the plane of the map. This interatomic line follows a valley in the electron density profile between the two large peaks resulting from the electron density concentrated around each nucleus. On either side of the interatomic surface the electron density is larger than on the surface. Along the interatomic line the electron density increases to a maximum value on the pass between the two peaks at the bond critical point before decreasing down the valley on the opposite side. By integrating the density in the region around each atom, as defined by the interatomic surfaces separating it from its neighbors, the electron population and hence the charge of the atom can be found. The atomic charges for the chlorides of the period 3 elements together with the bond critical point densities are given in Table 7 [14]. The charge on chlorine decreases steadily across the period but the charge on the central atom increases with the number of ligands to a maximum at $SiCl_4$ and then decreases to zero in Cl_2.

Table 7
Atomic charges and bond critical point densities for the period 3 chlorides

	ρ_b	q(Cl)	q(A)
NaCl	0.035	−0.87	−0.87
$MgCl_2$	0.057	−0.83	+1.65
$AlCl_3$	0.079	−0.78	+2.33
$SiCl_4$	0.106	−0.69	+2.77
PCl_3	0.120	−0.43	+1.29
SCl_2	0.133	−0.20	+0.40
Cl_2	0.140	0	0

3.3. Covalent and ionic character of bonds

The electron density at the bond critical point in $MgCl_2$ is very small and this observation coupled with the large charges on the atoms (Table 7) shows that the bonding in this molecule is predominately ionic. It seems reasonable to suppose that the major contributor to the force holding the two atoms together in this molecule is the attractive force between the two opposite charges, while the attraction due to the small electron density in the bonding region is weak. In SCl_2 the bond critical point density is much larger than in $MgCl_2$ while the charges on the atoms are relatively small. So in this molecule it is this concentration of density in the bonding region that is primarily responsible for the attractive force between the two atoms.

We see that for the chlorides in Table 7 the bond critical point density increases across the period. When this density is large and the charges on the atoms are small or zero, as in SCl_2 and Cl_2, the bond density accumulated in the bonding region is the major cause of the attraction between the two atoms and we describe the bonds as covalent. In contrast when this density is small and the charges are large, as in $MgCl_2$, we describe the bonds as predominately ionic. In $SiCl_4$ the bond critical point density is quite large and the atomic charges are also large, so the SiCl bond in $SiCl_4$ appears to have both a large covalent character and a considerable ionic character. It has usually been assumed that a large ionic character implies a small covalent character and vice versa but the analysis of electron density distributions shows that this is not always the case. It appears that a bond may have both a substantial ionic character and a substantial covalent character. However, there is some ambiguity in the term 'ionic character'. Based on the decreasing charge on the ligand from NaCl to Cl_2 we would say that the bonds are becoming less ionic but based on the increasing charge on the central atom from Na to Si we would conclude that the bonds are becoming more ionic. We will simply refer to this type of bond as a strongly polar bond. There are many bonds of this type including, for example, the bonds in BF_3, BCl_3, B_2O_3, SiF_4, $SiCl_4$ and SiO_2. Since the accumulated density in the bonding region and the atomic charges both make a substantial contribution to the attraction between the atoms these bonds are all very strong. They are considerably stronger, for example, than pure covalent bonds such as the C–C and Cl–Cl bonds.

The terms 'ionic' and 'covalent' only have a clear meaning in a limiting case. When the atomic charges are large and the bond critical point density approaches zero a bond can be described as ionic. When the atomic charges are very small or zero and the bond critical point densities large the bond may be described as covalent. Most bonds do not, however, fall into either of these two classes and can be described as polar, but they cannot be described as having a certain amount of covalent or ionic character.

3.4. The Laplacian of the electron density

We see only a slight bulge in the electron density in SCl_2 in the directions in which the lone pairs are expected. The lone pairs are, however, revealed much more

convincingly in the Laplacian of the electron density distribution. The Laplacian $\nabla^2\rho$ is the second differential of the density, ρ, in three dimensions:

$$\nabla^2\rho = \partial^2\rho/\partial x^2 + \partial^2\rho/\partial^2 y^2 + \partial^2\rho^2/\partial^2 z^2$$

It is convenient to plot the function $L(r) = -(h^2/4m)\nabla^2\rho$ which shows where the electron density is concentrated and where it is depleted with respect to the surrounding region [13] (Fig. 6). This is illustrated in Fig. 7 for a one-dimensional function $f(x)$ where we see that $-\mathrm{d}^2f(x)/\mathrm{d}x^2$ converts a small shoulder in the function $f(x)$ into a prominent maximum making it much more visible. The shoulder in $f(x)$ is a region where $f(x)$ is greater than $[f(x+\mathrm{d}x)+f(x-\mathrm{d}x)]/2$,

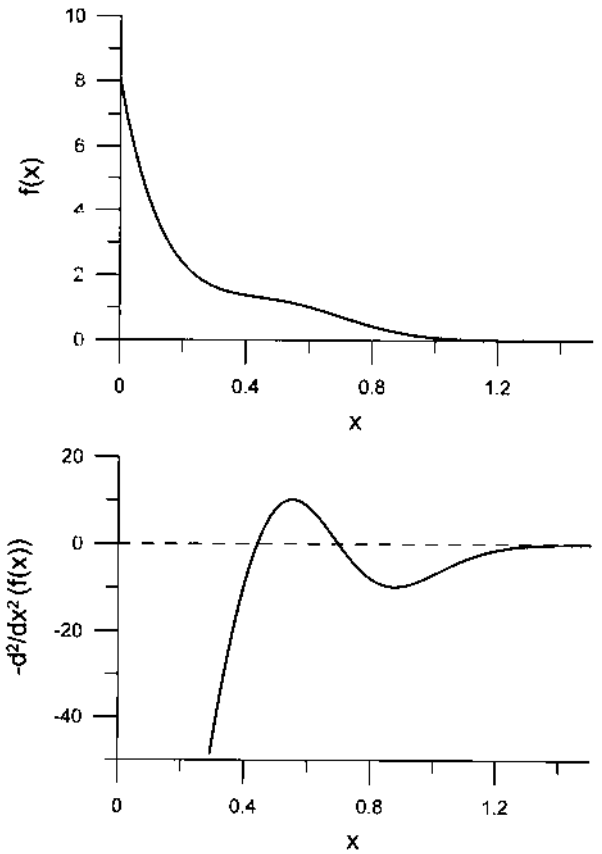

Fig. 7. Plot of a monatonically decreasing function $f(x)$, its second derivative $\mathrm{d}^2f(x)/\mathrm{d}x^2$, and the function $-\mathrm{d}^2f(x)/\mathrm{d}x^2$. This latter function has a maximum where $f(x)$ has a shoulder that is where $f(x)$ is locally concentrated.

that is, a region where $f(x)$ is locally concentrated. If we think of the three-dimensional electron density distribution as a cloud of negative charge of varying density then L shows where ρ is locally more dense, or concentrated, and where it is locally less dense or depleted. These regions of locally concentrated electron density are a consequence of the greater probability of finding an electron pair in this region than in the surrounding region.

We expect that the electron density will be locally concentrated in the directions in which lone pairs are located according the VSEPR model because of the increased probability of finding an electron pair in these directions. The contour map of $L(r)$ for SCl_2 (Fig. 6) clearly reveals the concentrations of electron density corresponding to the two lone pairs on the sulfur atom in SCl_2. Utilizing the analogy of a cloud of negative charge, these concentrations of electron density are usually called charge concentrations, in this case nonbonding charge concentrations. We also see a region of electron density concentration in the direction of each of the S–Cl bonds which are called bonding charge concentrations. The two bonding and two nonbonding charge concentrations have an overall tetrahedral arrangement. We see from Fig. 6 that a charge concentration corresponding to a lone pair occupies a larger area of an imaginary sphere lying in the valence shell of an atom than the concentration corresponding to a bonding pair which is more extended in the bond direction. The arrangement of the charge concentrations and their relative sizes correspond to the tetrahedral arrangement and relative sizes of the electron pair domains of the VSEPR model, thus providing support for the VSEPR model.

The electron density around the Cl ligands in SCl_2 is, like that around the S atom, not spherical. There is a slight bulge in the electron density of each Cl atom in a ring around the Cl atom and a region of charge concentration in $L(r)$ that has a toroidal (doughnut) shape. There are not three separate charge concentrations corresponding to three distinct lone pairs as expected from the Lewis model because there are not three localized lone pairs in the valence shell of the chlorine ligands. The most probable locations of the two sets of four same spin electrons are only brought into coincidence at one point by the formation of a single bonding pair. The remaining six electrons then have a most probable distribution in a continuous circle around the bond axis (Fig. 8). Localized lone pairs are not formed in the valence shell of singly bonded ligand and in linear molecules as has been pointed out by Linnett in his double-quartet model [15].

In contrast to the map of $L(r)$ for SCl_2, the map of $L(r)$ for $MgCl_2$ does not show any charge concentrations. Because almost all of the valence shell density of the Mg atom is transferred to the Cl atom, the $MgCl_2$ molecule consists essentially of an Mg^{2+} ion and two Cl^- ions. For the Mg^{2+} ion the plot of $L(r)$ shows only the spherical charge concentration corresponding to the inner core of the atom. The Cl^- ions show only a very nearly spherical charge concentration corresponding to the almost spherical valence shell density as well as a spherical charge concentration corresponding to the inner core. The linear geometry of this molecule results only

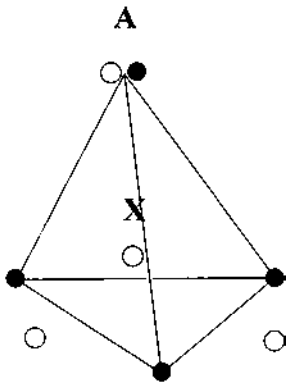

Fig. 8. Most probable arrangements of α and β spin electrons in the valence shell of a singly bonded ligand showing that only one localized bonding pair is formed while the nonbonding electrons are distributed in a circle.

from the repulsion between the two Cl ligands. In contrast, the angular geometry of SCl_2 is determined by the angular arrangement of the two bonding charge concentrations rather than by the repulsion between the two Cl ligands which is, however, a factor in determining the bond angle.

The analogous F_2O molecule has a similar angular geometry because the valence shell electrons of the oxygen atom are well localized into pairs by the electronegative fluorine ligands. In contrast, the valence shell electrons of the central oxygen atom in Li_2O are not localized into pairs by the weakly electronegative Li atoms and so the molecule has a linear geometry determined by the repulsion between the two Li ligands. Disiloxane, $(SiH_3)_2O$, represents an intermediate case between Li_2O and F_2O. The valence shell electrons of oxygen are rather poorly localized into pairs by the weakly electronegative silicon atoms. These poorly localized pairs have only a weak orienting effect on the ligands which does not compete very effectively with the repulsion between the Si ligands, so the bond angle of 140° is much larger than the tetrahedral value [11].

4. Summary and conclusions

Analysis of the electron density distribution of a molecule confirms the validity of the VSEPR model, in that it provides evidence for the electron density (charge) concentrations that correspond to the bond pair and lone pair domains of the VSEPR model. But it also shows that valence shell electrons are not always as localized into pairs as the VSEPR model assumes and thus helps us to understand some of the exceptions to the VSEPR model. The analysis of ρ gives us information about the shapes of atoms and groups in a molecule providing, for example, an explanation for the non-tetrahedral bond angles in a molecule such as $C(OH)_4$.

Moreover, the analysis of ρ provides values for atomic charges. These charges are important, for example, as they give insight into the nature of the bonding in many molecules, and they provide an understanding of the dependence of the intramolecular radius of a ligand on the atom to which it is attached.

The LCP model has many similarities to the VSEPR model except that it is expressed in terms of the concept of ligand–ligand repulsion instead of bond and lone pair repulsions. According to the VSEPR model molecular geometry is determined by the repulsive interactions of bond pairs and lone pairs. In terms of the LCP model lone pairs behave like pseudo-ligands because they occupy a certain portion of the valence shell of the central atom, thus prohibiting the attachment of ligands in this area. The LCP and VSEPR models generally predict the same geometry for molecules for which VSEPR is a valid model so it does not appear to be possible to distinguish between them. However, the LCP model does have the following advantages: (1) it explains the geometry of molecules when the VSEPR model breaks down because the ligands are not sufficiently electronegative to localize the electrons of the central atom into pairs. (2) It accounts for the increase in bond length with increasing coordination number. (3) It provides a more quantitative understanding of bond angles. (4) It accounts for the nontetrahedral angles at the central atom in molecules such as $C(OH)_4$ and $C(C_2H_5)_4$. (5) The existence of stereochemically inactive 'lone pairs', which cannot be explained by the VSEPR model, is consistent with the LCP model.

Acknowledgements

The author thanks Dr George Heard for assistance with the preparation of the Figures, Dr George Heard and Maggie Austen for valuable discussion and comments, and Dr Peter Robinson for his valuable collaboration over many years that helped to develop some of the ideas expressed in this review. The author also thanks the Natural Sciences and Engineering Council of Canada and the Petroleum Research Fund of the American Chemical Society for financial support.

References

[1] R.J Gillespie, I. Hargittai, The VSEPR Model of Molecular Geometry, Allyn and Bacon, Boston, 1991.
[2] R.J. Gillespie, E.A. Robinson, Angew. Chem. Int. Ed. Engl. 35 (1996) 495.
[3] E.A. Robinson, S.A. Johnson, T.-H. Tang, R.J. Gillespie, Inorg. Chem. 36 (1997) 3022.
[4] R.J. Gillespie, I. Bytheway, E.A. Robinson, Inorg. Chem. 37 (1998) 2811.
[5] R.J. Gillespie, E.A. Robinson, Adv. Mol. Struct. Res. 4 (1998) 1.
[6] L. Pauling, The Nature of the Chemical Bond, third ed., Ithaca, New York, 1961.
[7] L.S. Bartell, J. Chem. Phys. 32 (1960) 827.
[8] L.S. Bartell, Tetrahedron 17 (1962) 177.
[9] C. Glidewell, Inorg. Chim. Acta Rev. 7 (1973) 699.

[10] G.L. Heard, R.J. Gillespie, D.W.H. Rankin, J. Mol. Struct. (2000) in press.
[11] R.J. Gillespie, S.A. Johnson, Inorg. Chem. 36 (1997) 3031.
[12] A.R. Mhajoub, X. Zhang, K. Seppelt, Eur. J. Chem. 4 (1995) 261.
[13] (a) R.F.W. Bader, Atoms in Molecules: A Quantum Theory, Clarendon Press, Oxford, 1990. (b) R.F.W. Bader, Chem. Rev. 91 (1991) 893. (c) R.F.W. Bader, Acc. Chem. Res. 18 (1985) 9.
[14] G.L. Heard, R.J. Gillespie, unpublished results.
[15] J.W. Linnett, The Electronic Structure of Molecules, Wiley, New York, 1964.